International Journal of Nanomedicine

Dovepress
open access to scientific and medical research

Open Access Full Text Article

ORIGINAL RESEARCH

Pomegranate Juice Diminishes The Mitochondria-Dependent Cell Death And NF-kB Signaling Pathway Induced By Copper Oxide Nanoparticles On Liver And Kidneys Of Rats

This article was published in the following Dove Press journal:
International Journal of Nanomedicine

Eman I Hassanen[1,*]
AF Tohamy[2,*]
Marwa Y Issa[3,*]
Marwa A Ibrahim[4,*]
Khaled Y Farroh[5,*]
Azza M Hassan[1,*]

[1]Pathology Department, Faculty of Veterinary Medicine, Cairo University, Giza, Egypt; [2]Toxicology and Forensic Medicine Department, Faculty of Veterinary Medicine, Cairo University, Giza, Egypt; [3]Pharmacognosy Department, Faculty of Pharmacy, Cairo University, Giza, Egypt; [4]Biochemistry Department, Faculty of Veterinary Medicine, Cairo University, Giza, Egypt; [5]Nanotechnology Department, Agricultural Research Center, Giza, Egypt

*These authors contributed equally to this work

Background: Pomegranate (*Punica granatum* L) has been used since ancient times in the traditional medicine of several cultures, particularly in the Middle East. It is an essential commercial crop full of bioactive compounds with several medical applications. Pomegranate is very popular for its biological effects exerted by phenolic compounds via free radical scavenging abilities. It has revealed high antioxidant and anti-inflammatory activities and is beneficial for the amelioration of liver and kidney diseases.

Purpose: To elucidate the potential efficacy of pomegranate juice (PJ) against copper oxide nanoparticles (CuO-NPs)-induced apoptosis, inflammation, and oxidative stress damage.

Study design: 37 nm sized CuO-NPs were prepared by precipitation method and characterized by using X-ray diffractometer (XRD), Zetasizer nano-and high-resolution transmission electron microscope (HR-TEM). 30 Wistar rats were partitioned into 6 equal groups as follows: Group 1 (negative control), groups 2 & 3 (PJ control groups), group 4 (CuO-NPs group), groups 5 & 6 (CuO-NPs + PJ groups). Methods: Hepato-renal protective effect of PJ was evaluated by measuring levels of serum marker enzymes (ALT, AST,blood urea nitrogen and creatinine). Cu NPs bioaccumulation in liver and kidneys was determined by using atomic absorption spectrophotometer. The oxidative stress markers, Rt-PCR analysis, histopathological and immunohistochemical studies were carried out in the liver and kidneys to support the above parameters.

Results: Rats injected with CuO-NPs showed higher levels of the above serum marker enzymes, alteration of oxidant–antioxidant balance together with severe pathological alterations in liver and kidney tissues and overexpression of both caspase-3 and nuclear factor kappa B protein (NF-κB) associated with upregulation of Bax gene and downregulation of Bcl2 gene in these organs. PJ ameliorated all of the above toxicological parameters.

Conclusion: PJ was proved to be a potential hepato-renal protective agent against liver and kidney damage induced by CuO-NPs via its antioxidant, anti-inflammatory, and anti-apoptotic effects.

Keywords: apoptosis, nanoparticles, pomegranate, histopathology, gene

Introduction

Nanotechnology has shown a remarkable and rapid development related to its widespread applications in many fields, such as food industry, cosmetics, electronics, and medicine.[1,2] Lately, with the extensive use of nanoparticles (NPs), health hazards and ecological effects associated with NPs exposure have become of major

Correspondence: Marwa A Ibrahim
Biochemistry, Faculty of Veterinary Medicine, Cairo University
Email marwaibrahim@cu.edu.eg

submit your manuscript | www.dovepress.com
DovePress
http://doi.org/10.2147/IJN.S229461

attention.[3,4] Furthermore, NPs applications have been restricted due to the shortage of biosafety verification.[5] Thus, more assessment about their possible toxicity in vivo is required prior to any prospective applications.[6]

Copper (Cu) is a fundamental component essential for some normal physiological cellular functions, such as carbohydrate, protein, and xenobiotic metabolism, besides its role in the antioxidant defense system. Over the last few decades, the toxicity impacts of Cu and its compounds have been studied. Adverse effects and injurious impacts for liver, kidney, immune system and gastrointestinal tract were reported upon exposure to Cu intake that exceeds the range of biological tolerance.[7]Although the toxic effects of Cu and its compounds have been discussed, several studies reported gaps concerning the risk caused by Cu NPs.[8]

Metal oxide nanoparticles have attracted much attention because they can be used in numerous applications such as nanodevices, nanosensors, and catalysis.[9] However, these nanoparticles (NPs) are potential toxicants and few trials have been conducted to evaluate their toxicity in biological systems.[10] NPs of some metal oxides can pass through physiological barriers causing increased inflammatory responses, and can cause severe damage in DNA and protein structures, hence causing apoptosis and mutations.[11]

Copper and copper oxide nanoparticles (Cu NPs and CuO NPs, respectively), are extensively utilized as feed additives in poultry farms, plastic industry and lubricants for metallic coating.[12] Furthermore, Cu NPs exhibit potent antimicrobial effects against a variety of virulent microorganisms.[13]

CuO-NPs, similar to any of other NPs, enter the environment and human body via different ways through ingestion, inhalation, skin pores, reproductive and urinary tracts and accumulate in vital organs such as brain, liver, or kidneys.[14] NPs possess some health threats due to their small size, high surface-to-volume ratio, electronic properties, reactivity, functional groups and aggregation behavior.[9] NPs can pass through cell membranes and interact with the cellular and biological systems.[15] Consequently, NPs can cause harmful impacts on cellular functions.[16] The cytotoxic effects associated with Cu-based NPs are related to the increase in the reactive oxygen species (ROS) production.[17]

Herbs are well established as health beneficial foods and as a source for drug development. Herbal medicines derived from plant extracts are being progressively used for the treatment of many diseases such as liver and kidney diseases,[18] atherosclerosis, hypertension, diabetes mellitus and cancer.[19] It would be of great interest to explore natural products endowed with antioxidative potential that could prevent or reduce the induced toxicological alterations.

Pomegranate (*Punica granatum* L.) has been used since ancient times in the traditional medicine of several cultures, particularly in the Middle East. Pomegranate fruit, juice, and peel extracts are rich sources of polyphenols such as tannins, anthocyanins, and flavonoids and hence possess potent antioxidant properties.[20–22] Because of its potent antioxidant activity, pomegranate is considered as one of the commonly used natural antioxidants. The effectiveness and safety of its isolated antioxidants have been tested.[23] Murthy et al added that the methanolic extract of the peel has shown a higher antioxidant potential than that of the seeds and could prevent CCl_4-induced hepatotoxicity.[24] It is broadly stated that pomegranate displays antioxidant, anticancer, antivirus, antidiarrheal, antidiabetic, and antiproliferative activities.[25]

Despite, the widespread applications and the growing presence of Cu-containing nano products, there is only limited information on the potential risks of exposure to Cu-based NPs compared to other NPs. In spite of the presence of a few studies indicating that CuO-NPs can damage several organs we still lack data about the in-vivo toxicological effects of CuO-NPs in kidneys. In the current study, the nephrotoxic potential in addition to the hepatotoxic effect of CuO-NPs was investigated in rats. Besides, the possible antioxidant, anti-inflammatory and anti-apoptotic effect of PJ against CuO-NPs toxicity in rats. In this work, we report for the first time, to the best of our knowledge according to previous literature, the in vivo toxicity and bio-accumulation of CuO-NPs in liver and kidney tissues by conducting a short term, repeated dose toxicity study.

Materials And Methods

Chemicals

Copper (II) chloride dehydrate ($CuCl_2.2H_2O$, 99.999% Pure), ethanol ($C_2H_5OH \geq 99.8\%$ Pure), and sodium hydroxide pellets (NaOH, 99.99% Pure) were obtained from Sigma-Aldrich, the USA chemical company.

Preparation And Characterization Of Copper Oxide Nanoparticles

CuO-NPs were prepared by a chemical precipitation method utilizing copper (II) chloride dehydrates precursor salt.[26] Briefly, a solution of copper (II) chloride dihydrate (0.5M) in ethanol was prepared. Then, 100 mL of a

solution of sodium hydroxide solution (1M) in ethanol was added dropwise to the copper (II) chloride dihydrate solution under continuous stirring at room temperature. The color of the reaction mixture turned black. The copper oxide nanoparticles were separated and washed with ethanol and deionized water by centrifugation. The resulting precipitate was dried under vacuum at 50°C and annealed at 400°C for 4 hrs. The crystalline and phase structure of the prepared CuO-NPs were examined using X-ray diffractometer (XRD, X'Pert Pro, PanAlytical, Netherlands). Zeta potential and size of the prepared nanoparticles were determined by using Zeta sizer 3000HS (Malvern Instruments, UK). High-resolution transmission electron microscopy (HR-TEM, Tecnai G20, FEI, and the Netherlands) was used to determine the morphology and size of nanoparticles.

Plant Material

Pomegranate fruits were acquired from a local market in Cairo, Egypt. The authenticity of plant material was confirmed in the Botany Department, Faculty of Science, Cairo University, Giza, Egypt, through direct comparison with the herbarium samples and taxonomic properties.

Pomegranate Juice Preparation

Ten kilograms of Manfalouty pomegranate fruits were immediately washed, manually peeled and the skins covering arils were eliminated. Then, the juice was acquired from arils by mechanical press, without crushing the seeds (kernels) and stored at −18°C for no longer than two months until used for our experimental study.[27]

Sample Preparation For UPLC-ESI–QTOF-MS Analysis

The lyophilized pomegranate juice was mixed with 5 mL methanol (MeOH) containing umbelliferone (10 µg/mL) as internal standard, using a Turrax mixer (11,000 rpm) for five 20 s periods, separating each period with 1 min intervals to prevent heating, then the extracts were vortexed vigorously and centrifuged at 3000 rpm for 30 mins to remove debris and filtered using 22 µm pore size filter. An aliquot of 500 µL was placed on a (500 mg) C18 cartridge preconditioned with MeOH and H_2O. Samples were then eluted using 5 mL MeOH, the eluent was evaporated under a nitrogen stream, and the collected dry residue was resuspended in 500 µL MeOH. Three microliters of the supernatant were used for UPLC-MS analysis.

High-Resolution Ultra-Performance Liquid Chromatography-Mass Spectrometry Analysis (UPLC-ESI–QTOF-MS)

Chromatographic separation was completed on the ACQUITY UPLC system (Waters, Milford, MA) equipped with an HSS T3 column (100 × 1.0 mm, particle size 1.8 µm; Waters). The analysis was achieved using a dual gradient elution system at a flow rate of 150 µL/min: 0 to 1 min, isocratic 95% A (0.1 formic acid in water v/v), 5% B (0.1 formic acid in acetonitrile v/v); 1 to 16 min, linear from 5% to 95% B; 16 to 18 mins, isocratic 95% B; and finally, isocratic 5% B. Full loop injection volume (3.1 µL) was used. The system was coupled to a 6540 Agilent Ultra-High-Definition (UHD) Accurate-Mass Q-TOFLC/MS (Palo Alto, CA, USA) equipped with an ESI interface. Operating method: drying nitrogen gas temperature 325°C with a flow of 10 L/min; nebulizer pressure 20 psig; sheath gas temperature 400°C with a flow 12 L/min; capillary voltage 4000 V; nozzle voltage 500 V; fragment voltage 130 V; skimmer voltage 45 V; octa pole radio frequency voltage 750 V. Data acquisition (2.5 Hz) in profile mode was governed via Mass Hunter Workstation software (Agilent technologies). The spectra were acquired in the negative and positive ionization modes, over a mass-to-charge (m/z), range from 70 to 1100. The detection window was set to 100 ppm. Characterization of compounds was performed by the generation of the candidate formula with a mass accuracy limit of 10 ppm, and also considering RT (retention time), MS^2 data and reference literature.

Animals And Experimental Design

Thirty male albino Wistar rats (200 ± 20 g) were obtained from the department of veterinary hygiene and management's animal house, faculty of veterinary medicine, Cairo University, Egypt. Animals were housed in plastic cages and fed with standard commercial pelleted feed as well as supplying water adlibitum. They were inspected for health status and adapted to the laboratory environment for 14 days before use. The experimental procedures were performed according to the guidelines enclosed in the guide for the care and use of laboratory animals 8th edition 2012[28] and approved by the institutional animal care and use committee (IACUC) of Cairo University (protocol number: CU-II-F-40-18).

Rats were indiscriminately distributed into six equal groups, 5 rats each, and were intraperitoneally injected with CuO-NPs daily for 7 days and/or pomegranate juice

via oral gavage at 3 days before CuO-NPs injection and extended for 14 days as follows:

Group (1): Control (injected sterile normal saline by ip route, daily for 7 days).

Groups (2, 3) were given PJ (1 and 3 mL/kg/day) respectively according to previous recent studies.[29,30]

Group (4) was given CuO-NPs (50 mg/kg/day) (i.e., 1/10 of the LD_{50}).[31]

Groups (5, 6) were given both CuO-NPs and PJ by the same formerly mentioned doses.

Sampling

At the end of the experiments, rats were euthanized then liver and kidneys of each rat were collected. Some of the tissue specimens were stored in plastic bags at −80°C for evaluation of oxidative stress markers, Rt-PCR analysis, and determination of Cu content. The others were fixed in 10% neutral-buffered formalin solution for histopathology and immunohistochemistry.

Biochemical Tests

Alanine aminotransferase (ALT), aspartate aminotransferase (AST), blood urea nitrogen (BUN) and Creatinine (CRE) levels were measured in serum samples according to the instructions of the manufacturer kits (Biodiagnostic, Cairo, Egypt).

Histopathological Studies

Liver and kidney tissue specimens were fixed in 10% neutral-buffered formalin, handled by conventional method and sliced at 4.5 µm to acquire paraffin sections stained by H&E for histopathological assessments.[32]

For microscopic grading and scoring of hepato-renal injury, at least five microscopic areas were assessed.[33,34] The criteria used for liver damage were hepatocellular vacuolar degeneration, fatty changes, necrosis, and apoptosis. Renal scoring was investigated according to renal tubular epithelial cells vacuolization, necrosis, hyaline droplets, and casts. The pathological lesions were evaluated and scored as mild, moderate, and severe, on a scale of 0–4, as follows (0 = normal histology, 1 = <25%, 2 = 25%: 50%, 3 = 50%: 75%, 4= >75%).

Immunohistochemical Studies

Caspase-3 and nuclear factor Kappa B protein (NF-κB) expression were examined for the determination of both apoptosis and inflammation within the hepatic and renal tissue sections. Briefly, formalin-fixed paraffin-embedded tissue sections were deparaffinized, microwaved and then incubated with caspase-3 antibody or NF-κB antibody (Abcam, Ltd., USA) at 1/200 dilutions overnight at 4°C, then washed and incubated with Peroxidase Block (Sakura BIO) and reagent required for the detection of the antigen-antibody complex (Power-Stain 1.0 Poly HRP DAP Kit, Sakura, REF. 52–0017). The sections were treated with DAB chromogen substrate for 10 mins and then the slides were counterstained by Hematoxylin, examined under a light microscope and analyzed using Image J software to evaluate mean % area of caspase-3 protein expressions in different groups. In the case of NF-κB immunostaining, positive immunostaining nuclei were blindly counted in 5 random microscopic fields per 3 random sections per group at × 400 magnification.

Oxidative Stress Evaluation

Malondialdehyde (MDA),[35] and reduced glutathione (GSH) levels were measured in liver and kidney tissues homogenate[36] following the manufacturer kit instructions (Biodiagnostic, Cairo, Egypt).

Quantitative Real-Time PCR For Caspase-3 And Bcl-2 Protein Levels

Total RNA was isolated using the RNeasy Mini Kit (Qiagen) according to the guidelines of the kit manufacturer. Both the concentration and purity of the isolated mRNA were evaluated by Nanodrop1000 to select the samples which showed the ratio of OD260/OD280 among 1.8 and 2.0.[37] The reverse transcription reaction to synthesize the cDNA was performed using M-MuLV Reverse Transcriptase (Thermo Scientific). The primer sets for all the examined genes were designed using primer 3 software. Caspase 3, forward primer: 5′-GGAGCTTGGAACGCGAAGAA-3′, reverse primer:5′-ACACAAGCCCATTTCAGGGT-3′; Bcl-2 forward primer:5′-GGATCCAGGATAACGGAGGC-3′, reverse primer: 5′-ATGCACCCAGAGTGATGCAG-3′ ACTB: Forward primer: 5′-CCGCGAGTACAACCTTCTTG-3′, reverse primer: 5′-CAGTTGGTGACAATGCCGTG-3′. The quantitative real-time PCR reactions were done using the SYBR Green PCR Master Mix (Applied Biosystems). A negative control containing no template was used. All PCR reactions were done in duplicate using a Bio-Rad iCycler iQ system. The PCR program was: Denaturation at 95°C for 5 mins; followed by 50 cycles of 95°C, 20 s; 58°C, 20 sand 72°C, 30 s. The m-RNA level in each sample was normalized to the ACTB

gene which is used as the internal reference. The relative quantitation was calculated using MxPro software.[38]

Copper Oxide Nanoparticles Bioaccumulation In Liver And Kidney Tissues

Flame atomic absorption spectrophotometer (AAS 5 FL, Carl Zeiss Jena GmbH, Germany) was used to measure the contents of copper in the liver and kidney tissue homogenates.[39] Briefly, 0.5 g tissue samples were placed in microwave digestion vessels containing concentrated nitric acid and 30% H_2O_2 overnight, then they were heated in a microwave digestion system (ETHOS One; Milestone, Sorisole, Italy) till becoming completely digested and colorless. Afterwards, the samples were allowed to cool and the remaining solutions were diluted with 2% nitric acid.

Statistical Analysis

Statistical analysis was performed utilizing SPSS version 16.0 software (SPSS Inc., Chicago, IL, USA). Values were expressed as means ±SD. Comparison of means between several groups was performed by one-way analysis of variance (ANOVA) and independent-test was used to compare between two groups. Values were considered statistically significant at $p \leq 0.05$.

Results

Characterization Of Copper Oxide Nanoparticles

X-Ray Diffraction (XRD) Pattern Of CuO NPs

The XRD pattern of the synthesized CuONPs was shown in Figure 1A. Peaks at 2θ = 32.48°, 35.54°, 38.64°, 48.85°, 61.52°, 65.66, 66.34and 68.02° were assigned to (110), (−111), (111), (−202), (−113), (022), (−311) and (220) of CuO nanoparticles, indicating that the crystalline structure of synthesized Cu nanoparticles presented a hexagonal wurtzite structure (Zincite, JCPDS 04-005-4712).

Dynamic Light Scattering (DLS) Analysis

Hydrodynamic diameter and surface charge were assessed in the nanometer range by using DLS and zeta potential. The size and zeta of CuO NPs were 37.3 nm and 28.2 mV, respectively (Figure 1B and C).

High-Resolution Transmission Electron Microscopic (HR-TEM) Analysis

HR-TEM was used to determine the accurate particle size of synthesized CuO-NP. Transmission electron microscope images illustrated in Figure 1D, showed CuO nanoparticles with particle size in the range of 28.9–45.6 nm and nearly spherical-shaped particles.

UPLC-ESI–QTOF-MS Analysis Of Pomegranate Juice

The phytochemical characterization of pomegranate juice was accomplished using UPLC-ESI–qTOF-MS analysis. UPLC-ESI–qTOF-MS is a powerful technique in the characterization of complex herbal mixtures and is extensively used in research. It is useful in identifying compounds present in plants, by comparing mass spectrum acquired with those in the literature (tentative identification).

Pomegranate juice was subjected to UPLC-ESI–qTOF-MS analysis, which allowed the identification of a total of 105 compounds together with 35 unidentified ones. Organic acids mainly citric acid were the major class of compounds identified. Hydrolyzable tannins were also abundant phenolics identified in pomegranate juice. Non-colored flavonoids and anthocyanins were also available. Other compounds, such as triterpenes, lignans, and iridoid glycosides, were also observed (Figure 1E–H). The 105 identified compounds were recognized by the interpretation of their fragmentation patterns obtained from their mass spectra. Information in the literature was utilized for the complete evaluation of the juice.

As shown in Supplementary File (Table S1), three compounds were detected having m/z191$^-$of citric acid /isocitric acid isomers. Ten citric acid derivatives were also identified in pomegranate juice.m/z 169$^-$ ions from the mass analysis are an indication for the presence of gallic acid and ellagitannins were detected by losses of galloyl-moieties (m/z 152) yielding gallate 169$^-$. Gallotannins, formed of monomeric and dimeric galloyl moieties linked to a hexose sugar, were also detected. Two compounds showing the molecular ion m/z 331$^-$ and one displaying the molecular ion m/z 483$^-$ were observed and considered as gallotannins. m/z 301$^-$ ions evidenced for the presence of ellagic acid and ellagic acid derivatives in the pomegranate juice assessed. Different flavonoids were also detected as phlorizin, naringenin hexoside, dihydrokaempferol-hexoside, and naringin. Two phenolic acid derivatives were identified in the investigated pomegranate juice, vanillic acid-hexoside, and Syringic acid-O-hexoside. Anthocyanin derivatives as cyanidin, delphinidin, pelargonidin and their derivatives were tentatively identified using positive mode ionization as compared to the literature.

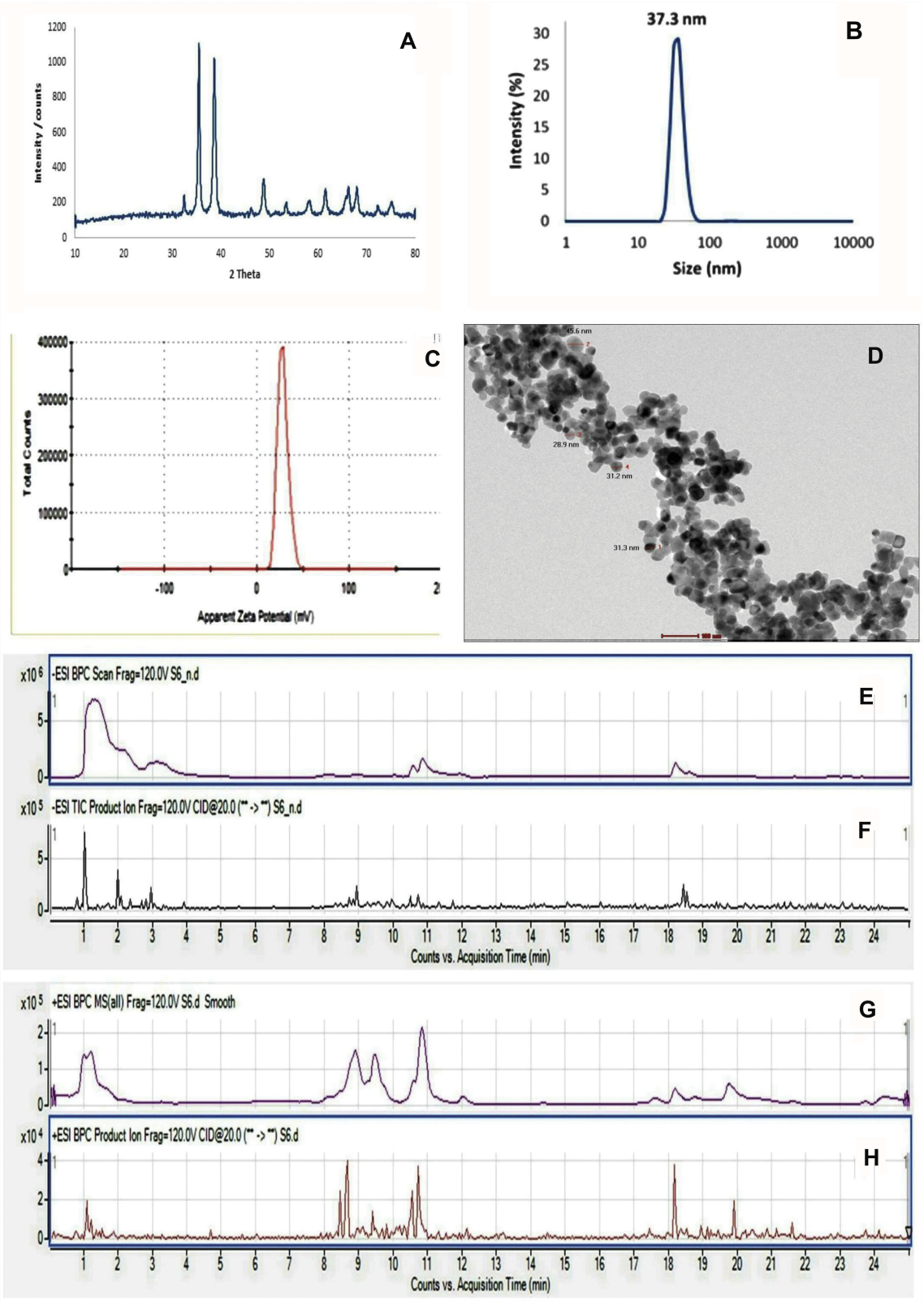

Figure 1 Characterization of the prepared nanoparticles and chemical analysis of PJ. (**A**) X-ray powder diffraction patterns of CuO-NPs. (**B** and **C**) Dynamic light scattering analysis of CuO-NPs showed: (**B**) Particle size with 37 nm and (**C**) Zeta potential 28.2 mV. (**D**) High-resolution transmission electron microscope image of CuO-NPs showed spherical NPs with particle size in the range of 28.8–45.6 nm. (**E** and **F**) UPLC-MS trace base peak (BPC) and production chromatograms of metabolite peaks detected in pomegranate juice negative mode. (**G** and **H**) Positive mode.

Biochemical Parameters

There was a significant elevation in ALT (Figure 2A), AST (Figure 2B), BUN (Figure 2C), and CRE (Figure 2D) levels in the group injected by CuO-NPs compared with the control group. On the other hand, there were remarkable improvements in such enzyme levels in the group treated with PJ either at low or high doses compared with CuO-NPs intoxicated group. Levels of the previous parameters in other groups were quite similar to each other.

Oxidative Stress Evaluations

The results in Figure 2E and F confirmed that rats intoxicated with CuO-NPs showed a significant elevation in MDA level together with a reduction in GSH level in liver and kidney tissue homogenates compared with the control group. Rats pretreated with either low or high doses of PJ showed better improvements manifested by a significant reduction in MDA levels with an elevation of GSH content compared with CuO-NPs intoxicated group.

Histopathological Examinations

Liver of rats in the control group showed normal hepatic parenchyma with normally arranged hepatocytes (Figure 3A). Meanwhile, the liver of CuO-NPs intoxicated rats revealed several degenerative changes as diffuse vacuolization of hepatocellular cytoplasm (Figure 3B) and fatty changes. There were sporadic hepatocellular necrosis and abundant apoptosis as well as the presence of intracytoplasmic eosinophilic globular inclusions (Figure 3C). Focal area of hepatocellular coagulative necrosis associated with mononuclear inflammatory cells infiltration was observed in some sections (Figure 3D). Treatment of rats with PJ revealed significant amelioration of the histopathological alterations in a dose-dependent manner. Mild cytoplasmic vacuolization with few apoptotic bodies was demonstrated in CuO-NPs/PJ 1mL/kg bwt group (Figure 3E). On the other side, the hepatocytes appeared greatly similar to those of normal group with sparse apoptotic figures observed in the group pretreated with 3 mL/kg bwt PJ (Figure 3F).

Kidneys of rats in the control group showed normal renal glomeruli and tubules (Figure 4A). In contrast, to the control group, remarkable renal pathological alterations were demonstrated in CuO-NPs intoxicated rats, varying from vacuolar degeneration of renal tubular epithelium to extensive renal tubular necrosis (Figure 4B). Necrotic tubular epithelium appeared with intensely eosinophilic cytoplasm and pyknotic or completely lysed nuclei associated with intraluminal aggregation of renal cellular and hyaline cast (Figure 4C and D). There were congestions of interstitial blood vessels and glomerular capillaries as well as peritubular hemorrhage in most sections. In addition, foci of regenerative renal tubules were also observed. Marked reduction of necrotic renal tubules with granular degeneration of renal tubular epithelium was demonstrated in the group receiving CuO-NPs and pretreated with 1 mL/kg bwt PJ (Figure 4E). Remarkable improvement was recorded in the group pretreated with 3 mL/kg bwt PJ, in which the renal tubules appeared normal in most sections with the presence of regenerative renal tubules which are lined with large basophilic vesicular nuclei (Figure 4F).

The results of the microscopic scoring of the hepato-renal injury (Figure 5) revealed severe histopathological alterations in both liver and kidney tissues in the group intoxicated with CuO-NPs. Moderate improvements in the observed pathological alterations were noticed in the group pretreated with 1 mL/kg bwt PJ. On the other hand, distinguished improvements were observed in the group pretreated with 3 mL/kg bwt PJ.

Immunohistochemical Examinations

Figures 6 and 7 notice the immunostaining expressions of caspase-3 and NF-κB proteins in the liver and kidney tissues obtained from rats in different experimental groups. The results revealed marked positive caspase-3 expression and extensive nuclear translocation of NF-κB protein within hepatocytes and renal tubular epithelium of rats in CuO-NPs group compared with the control group.

The mean percentage area of positive caspase-3 immunostaining reaction, as well as the percentage of-κB positive nuclei, were significantly reduced in groups pretreated either with low or high doses of PJ compared to CuO-NPs group as illustrated in Figure 8. Additionally, rats pretreated with 3 mL/kgbwt PJ showed better improvements in the previous immunostaining markers compared with those pretreated with 1 mL/ kg bwt PJ.

Quantitative Real-Time PCR For Caspase-3 And Bcl-2 Protein Levels

Up-regulation of caspase-3 mRNA levels together with down-regulation of Bcl-2 mRNA levels in liver and kidney tissue was noticed in the group intoxicated with CuO-NPs with significant difference compared with the control group. Groups pretreated with PJ either at low or high doses showed remarkable improvement manifested by a significant decline in caspase-3 mRNA levels and elevation in Bcl-2 mRNA

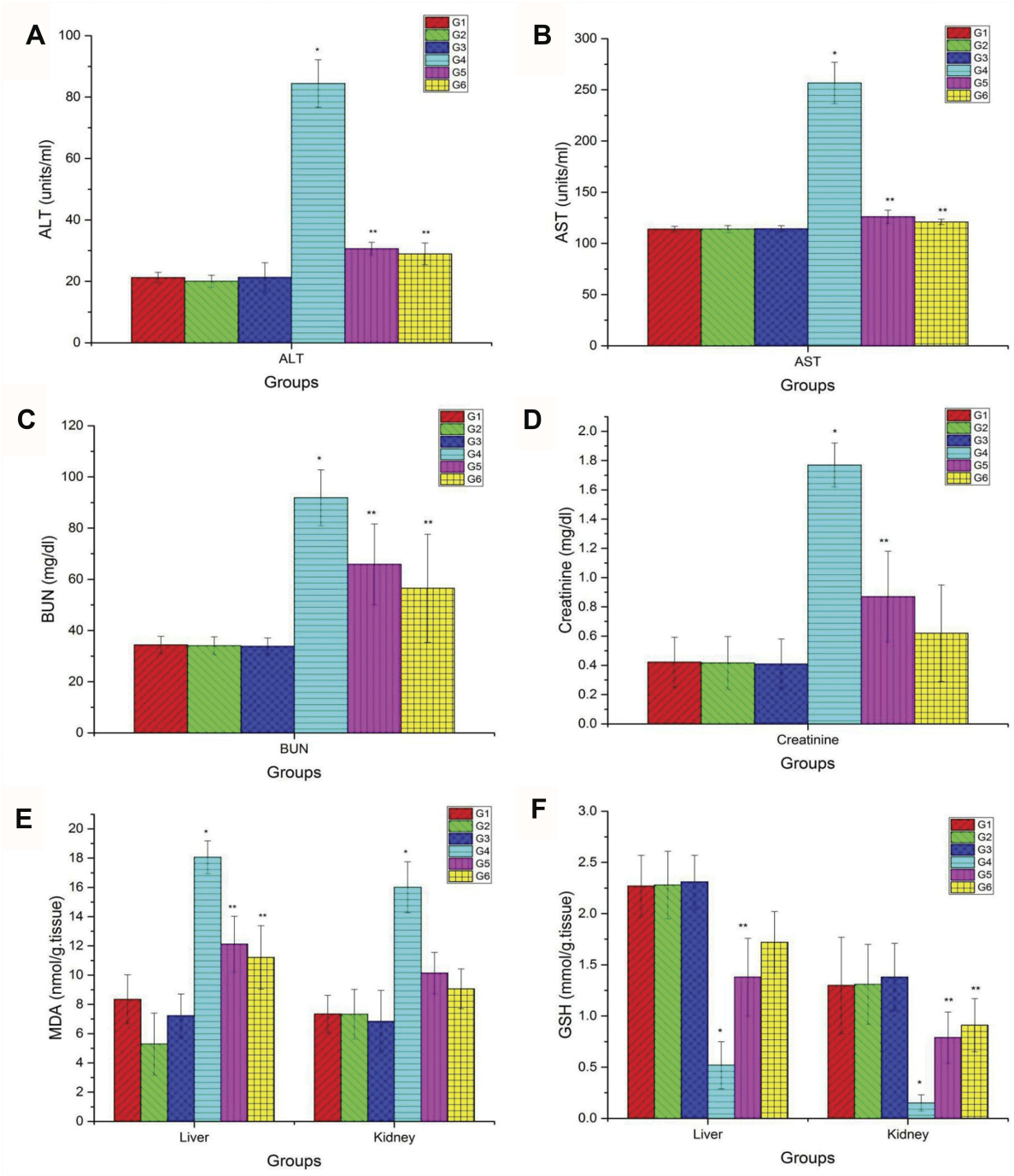

Figure 2 Blood biochemical tests and hepato-renal oxidative stress markers. (**A**) Serum levels of ALT, (**B**) AST, (**C**) BUN, (**D**) creatinine, (**E**) hepato-renal levels of MDA and (**F**) GSH levels in different groups. Data are represented as Mean ± SD. *Indicates significant difference from corresponding control group (G1) at $P \leq 0.05$. **Indicates significant difference from corresponding CuO-NPs group (G4) at $P \leq 0.05$.

Abbreviations: G1, control group; G2, group received 1 mL/kg bwt PJ; G3, group received 3 mL/kg bwt PJ; G4, group received CuO-NPs; G5, group received CuO-NPs + 1 mL/kg bwt PJ; G6, group received CuO-NPs + 3 mL/kg bwt PJ.

levels in liver and kidneys compared with CuO-NPs intoxicated group. Other experimental groups showed the same mRNA levels of the measured genes compared with the control group as noticed in Figure 9.

CuO-NPs Bioaccumulation In Liver And Kidney Tissues

The results in the Supplementary File Table (S2) showed a significant elevation in copper content in both liver and

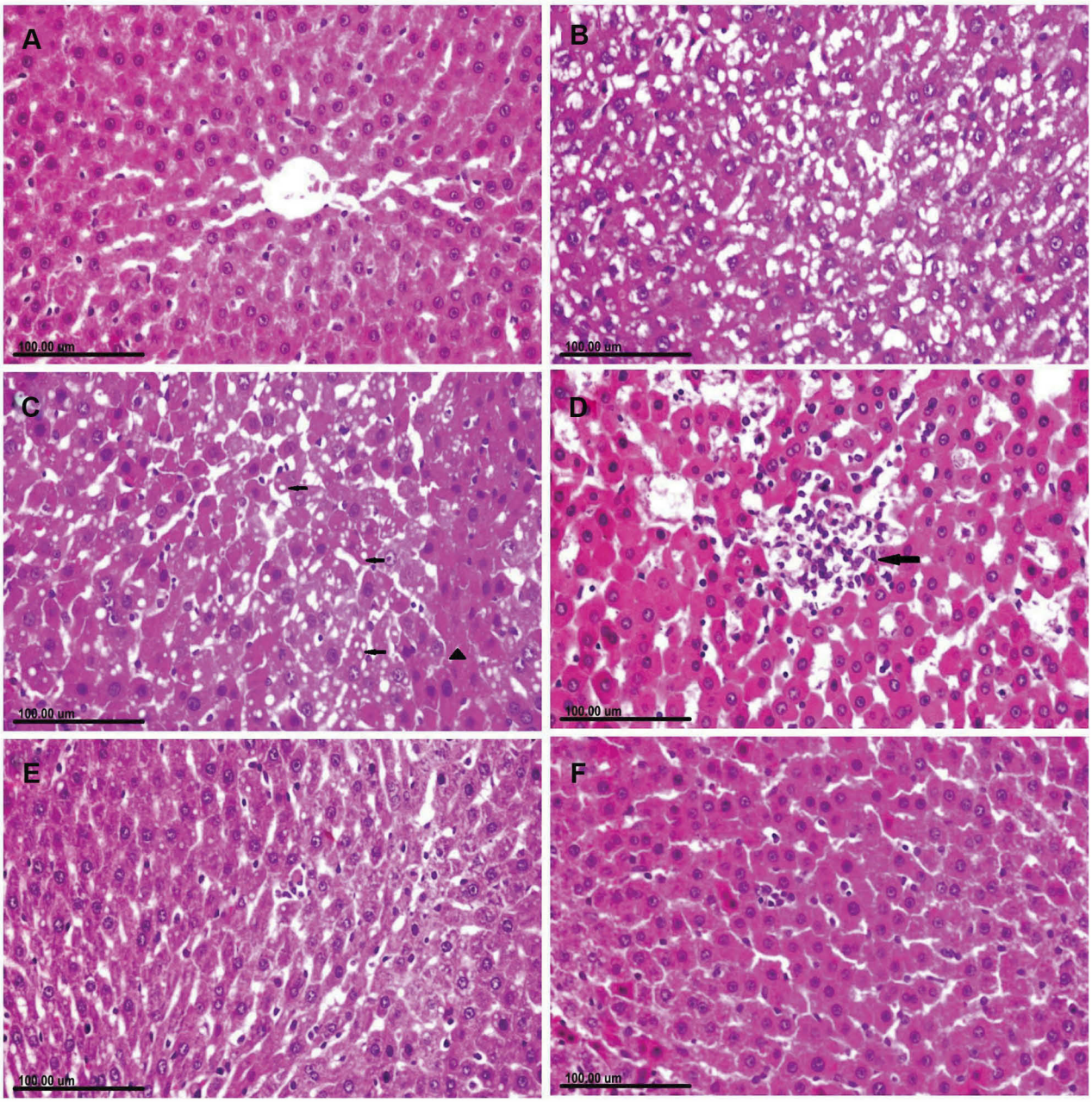

Figure 3 Photomicrograph of liver tissue sections stained with (H&E) of (**A**) normal rat showing normal hepatocytes. (**B**–**D**): CuO-NPs intoxicated rats showing. (**B**) Diffuse vacuolization of hepatocellular cytoplasm. (**C**) Cytoplasmic vacuolization (arrow) in some hepatocellular cells and sporadic necrosis (arrowhead) and abundant apoptosis in others as well as the presence of intracytoplasmic eosinophilic globular inclusions. (**D**) Focal area of coagulative necrosis infiltrated with mononuclear inflammatory cells (arrow). (**E**) CuO-NPs + 1 mL/kg bwt PJ group showing mild cytoplasmic vacuolization with few apoptotic bodies. (**F**) CuO-NPs + 3 mL/kg bwt PJ group showing normal hepatocytes with sparse apoptotic figures.

kidney tissues in CuO-NPs intoxicated group compared to the negative control group. Rats pretreated with PJ either with high or low doses showed a significant reduction in the copper content in liver tissues by 30% and 56% in rats pretreated with 1 and 3 mL/kg PJ, respectively, compared with CuO-NPs intoxicated group. Likewise, significant reduction in copper content was observed in kidneys of rats pretreated with 1 and 3 mL/kg PJ by 35 and 51%, respectively, compared with CuO-NPs intoxicated group. No significant differences were detected between other groups.

Discussion

Several reports confirmed that copper oxide nanoparticles (CuO-NPs) were extremely harmful in comparison with other nanoparticles.[40] Although the main target organs for

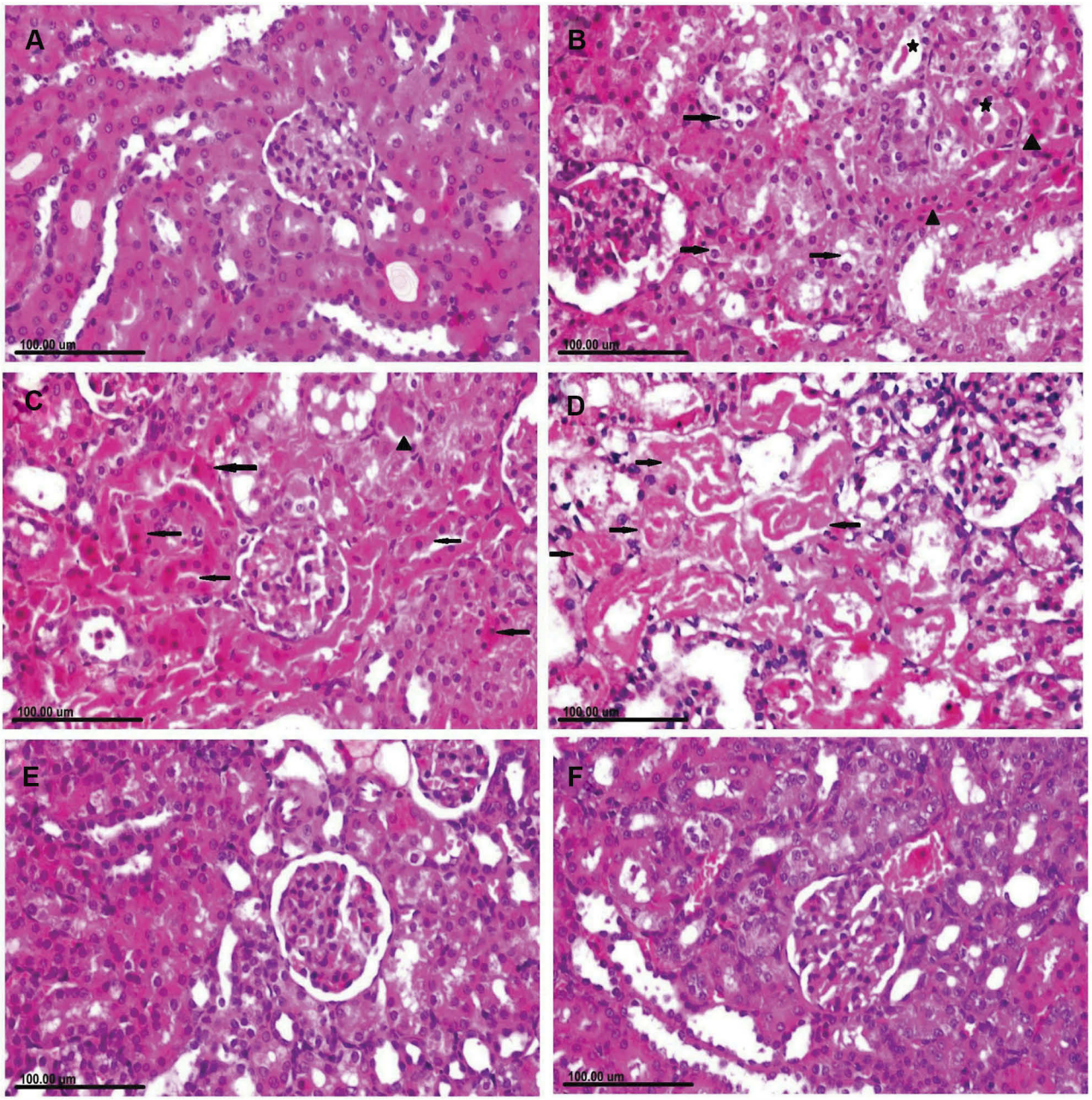

Figure 4 Photomicrograph of kidney tissue sections stained with H&E of (**A**) normal rat showing normal renal glomeruli and tubules. (**B**–**D**) CuO-NPs intoxicated rats showing (**B**) Cytoplasmic vacuolization (arrow) in some renal tubular epithelial cells and necrosis in other (arrowhead) associated with intraluminal hyaline cast (star). (**C**) Extensive renal tubular necrosis (arrow) with intensely eosinophilic cytoplasm and pyknotic nuclei with intraluminal aggregation of renal protein and cellular cast (arrowhead). (**D**) Necrotic tubular epithelium appearing with intensely eosinophilic cytoplasm and completely lysed nuclei (arrow) that are exfoliated in the tubular lumen. (**E**) CuO-NPs + 1 mL/kg bwt PJ group showing granular degeneration of renal tubular epithelium. (**F**) CuO-NPs + 3 mL/kg bwt PJ group showing regenerative renal tubules which are lined with large basophilic vesicular nuclei.

CuO-NPs toxicity are kidneys, liver, and spleen, few studies have been recorded about its in vivo toxic effects on the kidney tissue. Therefore, our study was designed to investigate the hepato-renal toxicity of CuO-NPs in rats, as well as, trail reduction of its toxicity using two different doses of pomegranate juice (PJ). This is the first study designed to evaluate the protecting impact of low (1 mL/kg) and high (3 mL/kg) doses of PJ against hepato-renal toxicity induced by CuO-NPs in rats.

Our findings confirmed a significant elevation in serum ALT and AST enzyme levels in the group of rats intoxicated with CuO-NPs indicating hepatocellular leakage and loss of the cell membranes integrity in the liver. There were also significant elevations in BUN and CRE in rats intoxicated

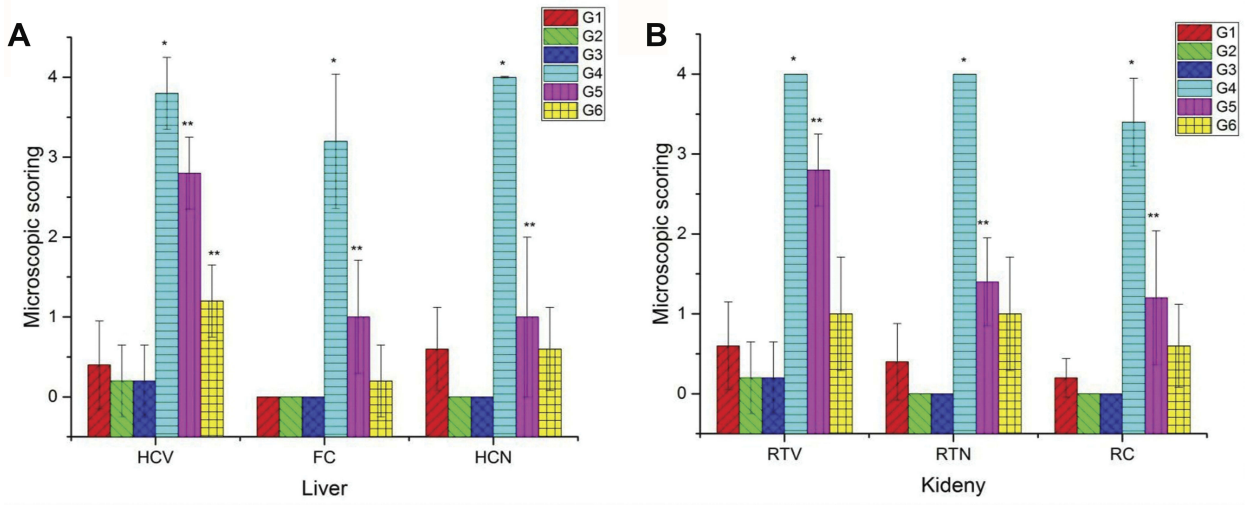

Figure 5 Microscopic scoring of both hepatic injury (**A**) and renal damage (**B**) in different groups. Data are represented as Mean ± SD. *Indicates significant difference from the corresponding control group (G1) at P ≤ 0.05 while **Indicates significant difference from the corresponding CuO-NPs group (G4) at P ≤ 0.05. Note: 0 = none, 1 = slight, 2 = mild, 3 = moderate, 4= severe tissue damage.

Abbreviations: G1, control group; G2, group received 1 mL/kg bwt PJ; G3, group received 3 mL/kg bwt PJ; G4, group received CuO-NPs; G5, group received CuO-NPs + 1 mL/kg bwt PJ; G6, group received CuO-NPs + 3 mL/kg bwt PJ; HCV, hepatocellular vacuolization; FC, fatty change, HCN, hepatocellular necrosis; RTV, renal tubular vacuolization; RTN, renal tubular necrosis; RC, intraluminal hyaline droplets and cast.

with CuO-NPs indicating renal damage. The results of hepato-renal profile enzymes clearly depict that CuO-NPs are extremely cytotoxic for both liver and kidney tissues. Similar previously reported findings confirmed that kidney and liver were counted among the first target organs of CuO-NPs toxicity.[9] Cu NPs with high reactivity interacted with and damaged the liver and kidney microscopic pictures and altered the hepato-renal serum enzyme profile.[41]

Histopathological examination and copper bioaccumulation results displayed severe hepato-renal degeneration and necrosis which altered the organ functions. Moreover, marked elevation in Cu content in liver and kidney tissues was noticed in CuO-NPs intoxicated group. The extent of degeneration within the liver and kidneys of CuO-NPs intoxicated rats was severe and might possibly alter the hepatic and renal functions. Nanoparticles get accumulated in the liver and alter the normal homeostasis of minerals leading to hepatocellular swelling and vacuolar degeneration. The hypercellularity of the glomeruli was incapable to filter the toxic substances leading to the buildup of the harmful products within the locality.[42] The same finding was reported in adult mice.[43] There were vacuolar degenerations and necrosis in the renal tubular epithelium of CuO-NPs intoxicated rats. These changes were a direct result of imbalance and disturbances in the homeostasis of kidney cells.[44]

Our results regarding the bioaccumulation of CuO-NPs showed excessive Cu contents in liver and kidney tissues of rats intoxicated with CuO-NPs compared to control group, while the accumulation of Cu in kidneys was higher than those in the liver tissue. The large bioaccumulation of CuO-NPs within the liver might be associated with the fenestrated, discontinuous endothelium of the hepatic sinusoids and blood vessels which permits the entry of the circulating NPs less than 100 nm into the hepatic parenchyma via opsonization.[45] The accumulation of nanoparticles may vary according to their solubility. Thus, we have a tendency to suggest that kidneys accumulate copper in the ionic form after the nanoparticles in vivo dissolution. So that, both mechanisms (phagocytosis and dissolution of Cu-ions) justify copper accumulation in the liver and kidneys of rats exposed to CuO-NPs.

The hepatotoxicity and nephrotoxicity induced by CuO-NPs were related to oxidative stress damage on the liver and kidney tissues[46] by triggering reactive oxygen species (ROS) production.[47] In the current study, rats intoxicated with CuO-NPs showed decreased levels of GSH antioxidant besides increasing levels of MDA; a product of lipid peroxidation, thereby implying that CuO-NPs not only generate ROS but also block cellular antioxidant defenses.[48] Oxidative stress was stated to be a vital mechanism of toxicity associated with NPs.[49] Significant elevation in MDA levels and decline in SOD antioxidant activity in liver of rats receiving CuO-NPs, as well as, oxidative stress damage and apoptosis in kidney tissue of nano-Cu receiving rats were stated.[50,51]

Oxidative stress is considered as the main predisposing factor related to programmed cell death.[52] Therefore, the mechanism of CuO-NPs-induced apoptosis may be

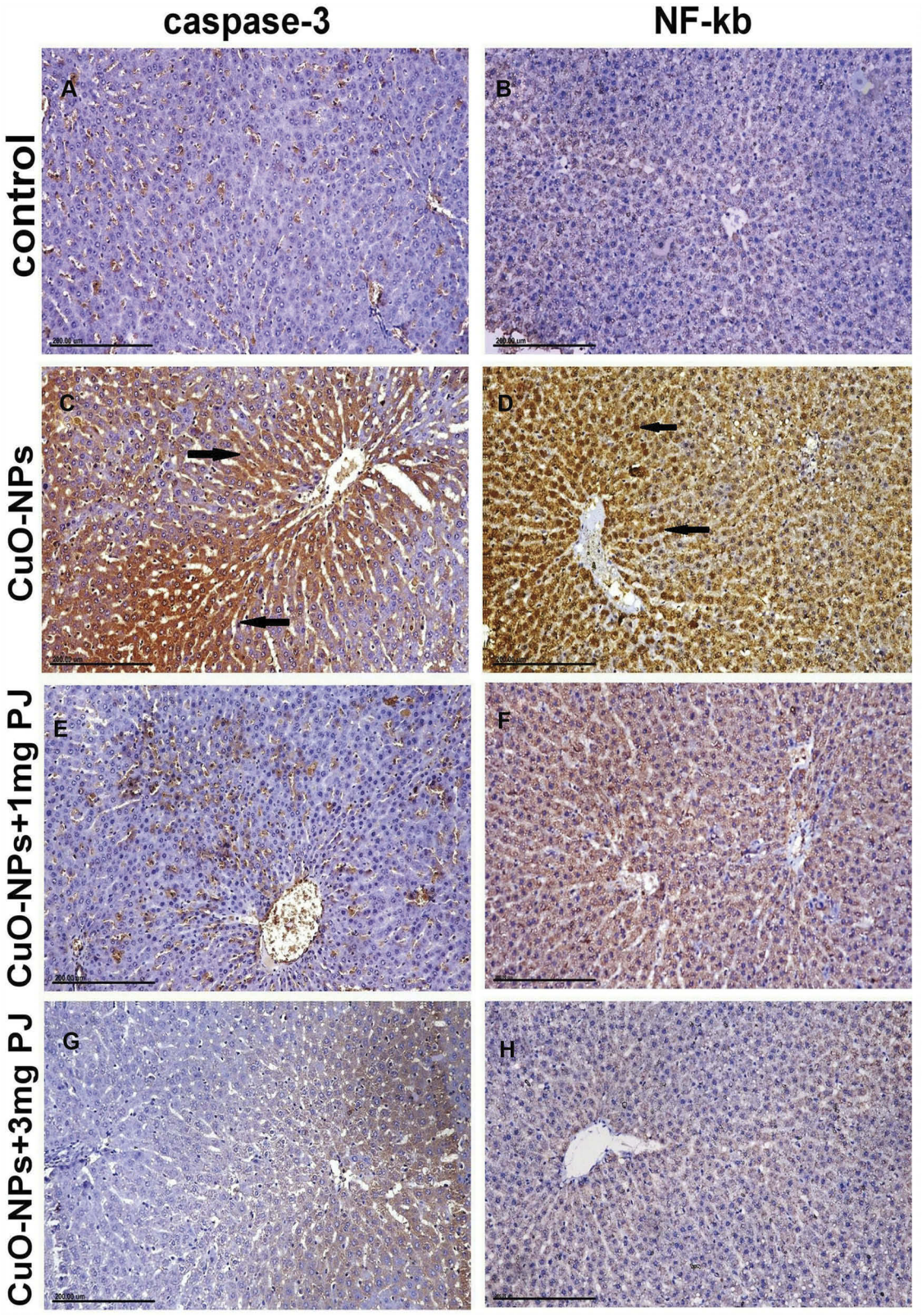

Figure 6 Immunohistochemical expression of caspase-3 and NF-κB protein in the liver sections in different groups showing (**A** and **B**) mild to negative Caspase-3 and NF-κB protein expression in control negative group. (**C** and **D**) Strong positive caspase-3 and extensive nuclear translocation of NF-κB protein within hepatocytes in the group intoxicated with CuO-NPs. (**E** and **F**) Moderate positive caspase-3 and NF-κB protein expression in the group pretreated with 1 mL/kg bwt PJ. (**G** and **H**) Mild to negative caspase-3 and NF-κB protein expression in the group treated with 3 mL/kg bwt PJ.

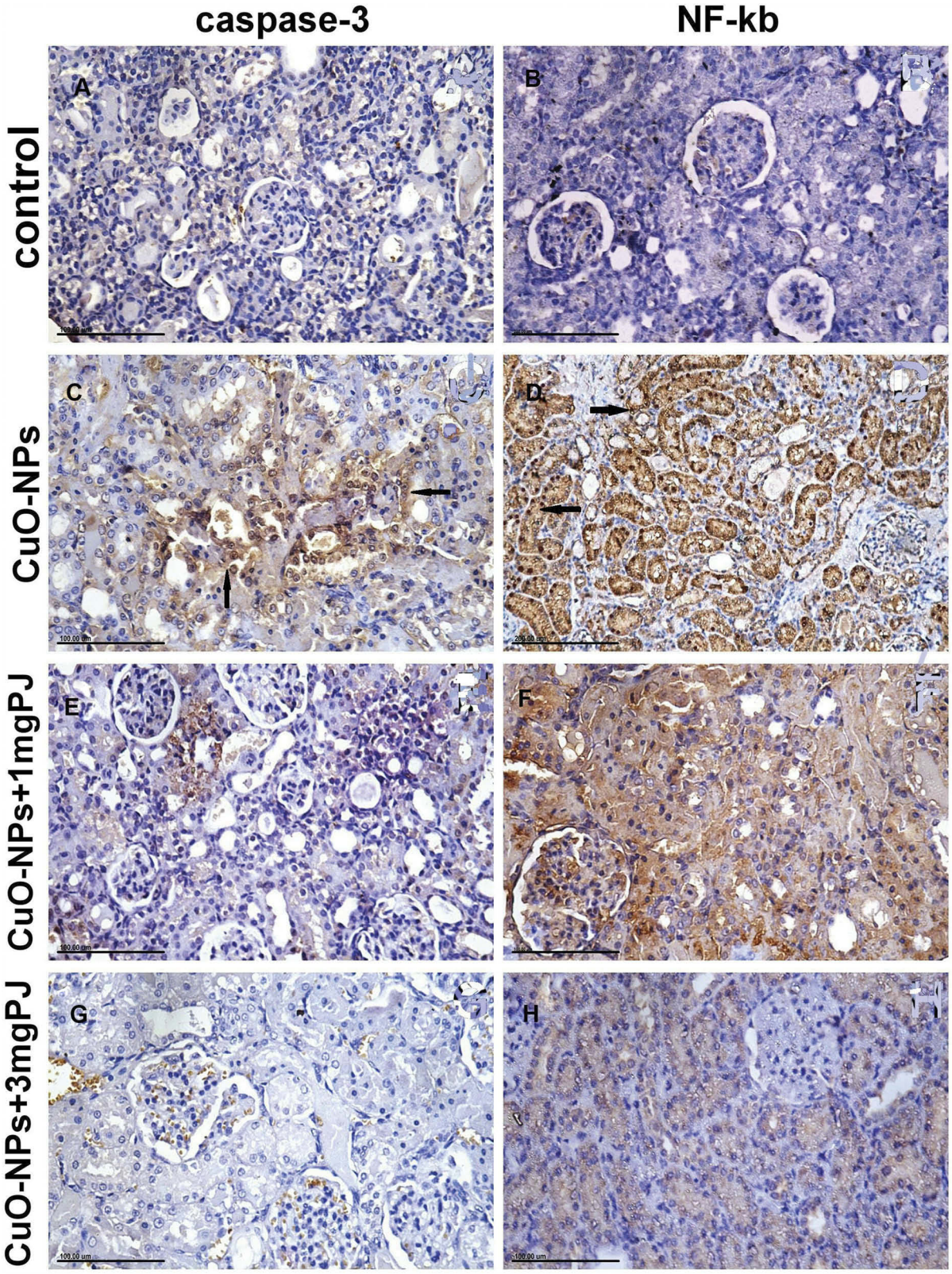

Figure 7 Immunohistochemical expression of caspase-3 and NF-κB protein in the kidney tissue sections in different groups showing (**A** and **B**) mild to negative caspase-3 and NF-κB protein expression in control negative group. (**C** and **D**) Moderate positive caspase-3 and extensive nuclear translocation of NF-κB protein within the renal tubular epithelial cells in the group intoxicated with CuO-NPs. (**E** and **F**) Mild to moderate positive caspase-3 and NF-κB protein expression in group pretreated with 1 mL/kg bwt PJ. (**G** and **H**) Mild to negative caspase-3 and NF-κB protein expression in group treated with 3 mL/kg bwt PJ.

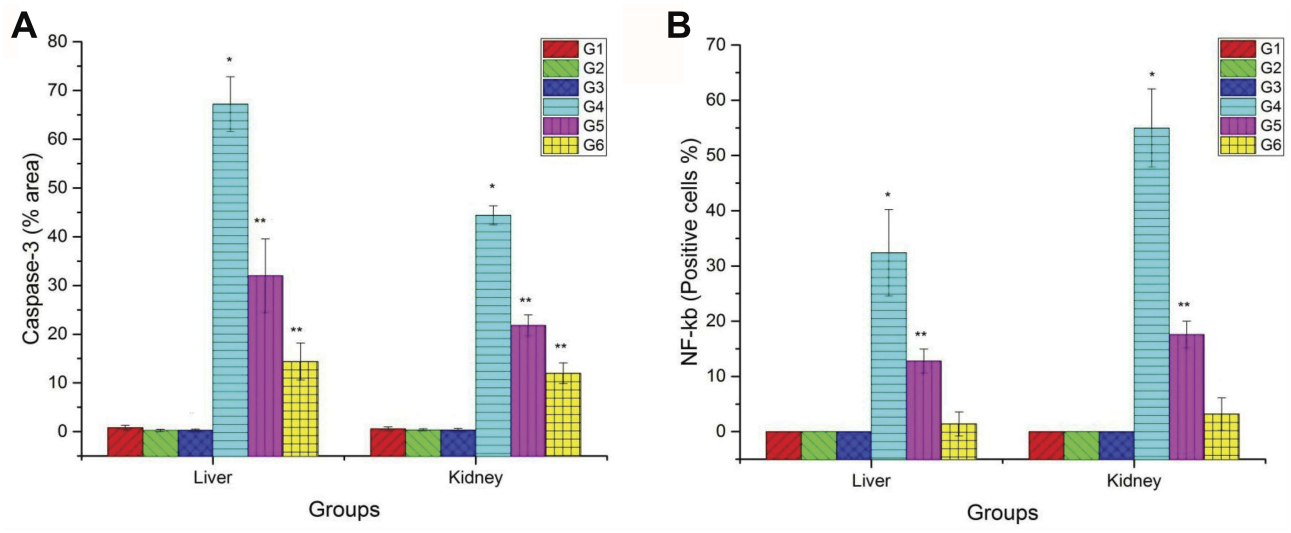

Figure 8 Bar chart representing (**A**) the mean % area of caspase-3 immunopositivity in the liver and kidney tissue sections. (**B**) Percentage of NF-κB immunopositive nuclei within hepatocytes and renal tubular epithelium of rats in different groups. Values represented as Mean ± SD. *Indicates significant difference from the corresponding control group (G1) at P ≤ 0.05. **Indicates significant difference from the corresponding CuO-NPs group (G4) at P ≤ 0.05.
Abbreviations: G1, control group; G2, group received 1 mL/kg bwt PJ; G3, group received 3 mL/kg bwt PJ; G4, group received CuO-NPs; G5, group received CuO-NPs + 1 mL/kg bwt PJ; G6, group received CuO-NPs + 3 mL/kg bwt PJ.

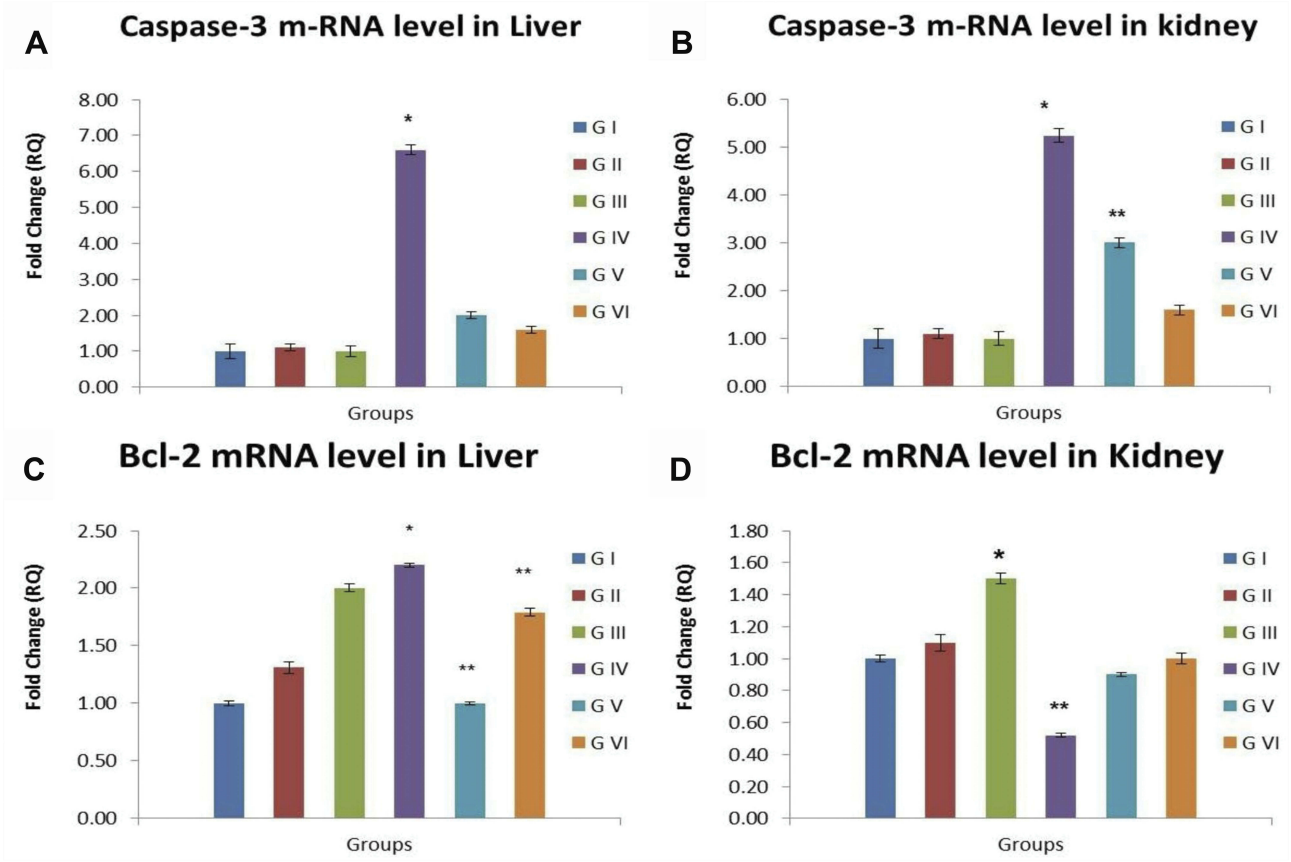

Figure 9 Bar chart representing (**A**) caspase-3 m RNA level in liver, (**B**) caspase-3 m RNA level in kidneys, (**C**) Bcl-2 m RNA level in liver, (**D**) Bcl-2 m RNA level in kidneys. Values represented as Mean ± SD. *Indicates significant difference from the corresponding control group (G1) at P ≤ 0.05. **Indicates significant difference from the corresponding CuO-NPs group (G4) at P ≤ 0.05.
Abbreviations: G1, control group; G2, group received 1 mL/kg bwt PJ; G3, group received 3 mL/kg bwt PJ; G4, group received CuO-NPs; G5, group received CuO-NPs + 1 mL/kg bwt PJ; G6, group received CuO-NPs + 3 mL/kg bwt PJ.

mediated by the mitochondrial-initiated pathway.[53] Two main signaling pathways controlled the mechanism of apoptosis, either mitochondrial or death receptor-mediated pathways which trigger a cascade reaction.[54] Pro-apoptotic proteins (Bax and caspase-3) and antiapoptotic protein (Bcl-2) are often demonstrated as necessary components of mitochondrial-mediated apoptosis.[55] Once the mRNA level of Bcl-2 protein declines and Bax protein rises, mitochondrial membrane disintegration happens leading to release of cytochrome C to the cytosol. Then, cascade reactions occur, which incorporates cytochrome binding with Apaf-1 leading to activation of caspase-9 and caspase-3. Several studies suggest that CuO-NPs trigger both apoptotic pathways initiated by oxidative stress in kidneys.[51] Similarly, our findings indicated down-regulation in Bcl-2 and up-regulation in caspase-3 mRNA levels in liver and kidneys of rats intoxicated with CuO-NPs. The immunohistochemical staining results showed overexpression of caspase-3 protein in liver and kidneys of rats intoxicated with CuO-NPs. In vitro studies confirmed that CuO-NPs enhanced apoptosis by increasing caspase-3 cleavage in some cells as human MCF7 breast cancer cells and HepG2 cells.[56] In rats, CuO-NPs mediated apoptosis via up-regulation of caspase-3 mRNA levels[57] and the upsurge in the gene expression ratio of Bax/Bcl2.[58] Semisch et al[59] confirmed that mitochondrial membrane damage may be caused by either direct interactions with the CuO-NPs or ROS-release leading to discharge of apoptotic enzymes.

NF-κB is a transcription factor and is considered as the main regulator of κB light chain expression in mature B lymphocytes and plasma cells.[60] The activation of NF-κB signaling pathway has an important role in the immune and inflammatory responses, and apoptosis.[61] Some metal oxide nanoparticles enhance the activation of NF-κB pathways.[62] Excessive ROS generation enhances pro-inflammatory cytokines via activation of NF-κB signaling pathway that controls transcription of inflammatory genes,[63] and release of IκBs leading to nuclear translocation of NF-κB.[64] Within the nucleus, NF-κB triggers transcription of proinflammatory mediators leading to inflammation, oxidative stress and apoptosis.[65,66]

Lately, naturally occurring anti-inflammatory, anti-apoptotic and antioxidant compounds influencing humans and animals health have gained considerable attention.[67] Our study was designed to evaluate the possible protective effect of PJ against hepato-renal toxicity induced by CuO-NPs.

The protective effect of pomegranate may be related to its phenolic compounds-comprising phenolic acids, tannins, flavonoids (anthocyanins),[68,69] these compounds are found in considerable amounts in the peels and juice of pomegranate fruits.[70] In the present study, pretreatment of rats with PJ showed better improvements in all of the above-mentioned toxicopathological parameters. Our results with the PJ were in accordance with previous reports confirming that pomegranate juice has strong antioxidant activity correlated to flavonoids especially anthocyanins subgroup in pomegranate.Their electron-deficient chemical structure makes them extremely reactive toward free radicals, making them potent natural antioxidants.[71] Moreover, anthocyanidins, which vary from other flavonoids, apart from flavan-3-ol, by lacking a carboxyl group in the C-ring, inhibit lipid peroxidation of liposome or cell membranes.[72] Pomegranate is rich in the three non-methylated anthocyanidins (cyanidin, delphinidin, and pelargonidin) and their 3-glucosides and 3,5-glucosides.[73] The antioxidant power of pomegranate juice is 3 times more than green tea and possess more total phenolics concentration, related to other fruit juices (apple, orange, cranberry, grape, grapefruit, and pineapple).[74]

Several studies confirmed the scavenger and antioxidant effect of PJ in the liver of rats after exposure to CCl_4.[75] Pomegranate juice was able to prevent the oxidative stress damage induced by CuO-NPs in liver and kidneys. Furthermore, its preventive effect was also observed at the histological levels that showed significant improvements in all of the histopathological parameters observed in both liver and kidney tissue sections. The presence of polyphenols in PJ might be involved in ameliorating the tissue damage induced by CuO NPs.[76] Moreover, PJ could reverse the progression of the pathological lesions by its strong antioxidant capacity, enhanced biological actions of nitric oxide, decreased inflammation and decreased angiotensin-converting enzyme activity.[77]

Another area of potential therapeutic interest of PJ is related to its anti-inflammatory and anti-apoptotic activity. Our results proved that pretreatment of rats by PJ exhibited mild to negative immunohistochemical staining of caspase-3 and NF-κb protein expression, as well as, better regulation in caspase-3 and Bcl2 protein levels in both liver and kidney tissues. Pomegranate is rich in several antioxidants including citric acid, tannins, anthocyanins, phenols and flavonoids which can directly or indirectly reduce oxidative damage by preventing the excessive generation of free radicals.[78] Pomegranate juice may be of

therapeutic potential for the treatment of several inflammatory diseases via decreasing the activation NF-κB in activated human mast cells and basophils.[79] Treatment of rats with PJ increased Bcl-2 expression and decreased caspase-3 expression then reduced oxidative stress damage and inflammatory reactions. These anti-apoptotic, antioxidant and anti-inflammatory effects of PJ may be the basis for its protection against pathological alterations in liver and kidney tissues.

Conclusion

Our study clearly suggested that pomegranate juice exerts dose-dependent therapeutic effects via its anti-apoptotic, antioxidant and anti-inflammatory effects. It ameliorated the oxidative stress damage induced by CuO-NPs in the liver and kidney tissues and regulated caspase-3, Bcl-2 levels, and NF-κB immunostaining expression. Additionally, PJ alleviated most of the histopathological lesions induced by CuO-NPs in liver and kidney tissue sections. From our findings, we have a tendency to recommend using pomegranate juice in human and animal nutrition for all of these functions and benefits.

Abbreviations

ALT, Serum alanine aminotransferase; AST, Serum aspartate aminotransferase; BUN, blood urea nitrogen; CRE, Creatinine; Cu NPs, copper nanoparticles; CuO-NPs, copper oxide nanoparticles; HR-TEM, high-resolution transmission electron microscope; NF-κB, nuclear factor kappa B protein; PJ, pomegranate juice; XRD, X-Ray diffractometer.

Author Contributions

All authors contributed to data analysis, drafting or revising the article, gave final approval of the version to be published, and agree to be accountable for all aspects of the work.

Disclosure

The authors report no conflicts of interest in this work.

References

1. Bhattacharya S, Alkharfy KM, Janardhanan R, Mukhopadhyay D. Nanomedicine: pharmacological perspectives. *Nanotechnol Rev*. 2012;1(3):235–253. doi:10.1515/ntrev-2011-0010
2. Khalaf AA, Hassanen EI, Azouz RA, et al. Ameliorative effect of zinc oxide nanoparticles against dermal toxicity induced by lead oxide in rats. *Int J Nanomedicine*. 2019;14:7729–7741. doi:10.2147/IJN.S220572
3. Johnson BM, Fraietta JA, Gracias DT, et al. Acute exposure to ZnO nanoparticles induces autophagic immune cell death. *Nanotoxicology*. 2015;9(6):737–748. doi:10.3109/17435390.2014.974709
4. Hassanen EI, Khalaf AA, Tohamy AF, Mohammed ER, Farroh KY. Toxicopathological and immunological studies on different concentrations of chitosan-coated silver nanoparticles in rats. *Int J Nanomedicine*. 2019;14:4723. doi:10.2147/IJN.S207644
5. Galdiero S, Falanga A, Vitiello M, et al. Silver nanoparticles as potential antiviral agents. *Molecules*. 2011;16(10):8894–8918. doi:10.3390/molecules16108894
6. Jang GH, Hwang MP, Kim SY, Jang HS, Lee KH. A systematic in-vivo toxicity evaluation of nanophosphor particles via zebrafish models. *Biomaterials*. 2014;35(1):440–449. doi:10.1016/j.biomaterials.2013.09.054
7. ATSDR U. Toxicological profile for copper. 2004.
8. Meng H, Chen Z, Xing G, et al. Ultrahigh reactivity provokes nanotoxicity: explanation of oral toxicity of nano-copper particles. *Toxicol Lett*. 2007;175(1–3):102–110. doi:10.1016/j.toxlet.2007.09.015
9. Chen Z, Meng H, Xing G, et al. Acute toxicological effects of copper nanoparticles in vivo. *Toxicol Lett*. 2006;163(2):109–120. doi:10.1016/j.toxlet.2005.10.003
10. Ahamed M, Alhadlaq HA, Khan M, Karuppiah P, Al-Dhabi NA. Synthesis, characterization, and antimicrobial activity of copper oxide nanoparticles. *J Nanomater*. 2014;2014:17. doi:10.1155/2014/637858
11. Adam N, Vakurov A, Knapen D, Blust R. The chronic toxicity of CuO nanoparticles and copper salt to Daphnia magna. *J Hazard Mater*. 2015;283:416–422. doi:10.1016/j.jhazmat.2014.09.037
12. Rim K-T, Song S-W, Kim H-Y. Oxidative DNA damage from nanoparticle exposure and its application to workers' health: a literature review. *Saf Health Work*. 2013;4(4):177–186. doi:10.1016/j.shaw.2013.07.006
13. Ebrahimnia-Bajestan E, Niazmand H, Duangthongsuk W, Wongwises S. Numerical investigation of effective parameters in convective heat transfer of nanofluids flowing under a laminar flow regime. *Int J Heat Mass Transf*. 2011;54(19–20):4376–4388. doi:10.1016/j.ijheatmasstransfer.2011.05.006
14. Das R, Gang S, Nath SS, Bhattacharjee R. Linoleic acid capped copper nanoparticles for antibacterial activity. *J Bionanosci*. 2010;4(1–2):82–86. doi:10.1166/jbns.2010.1035
15. Janrao K, Gadhave M, Banerjee S, Gaikwad D. Nanoparticle induced nanotoxicity: an overview. *AJBPS*. 2014;4(32):1. doi:10.15272/ajbps.v4i32.480
16. Keller AA, Wang H, Zhou D, et al. Stability and aggregation of metal oxide nanoparticles in natural aqueous matrices. *Environ Sci Technol*. 2010;44(6):1962–1967. doi:10.1021/es902987d
17. Misra SK, Nuseibeh S, Dybowska A, et al. Comparative study using spheres, rods and spindle-shaped nanoplatelets on dispersion stability, dissolution and toxicity of CuO nanomaterials. *Nanotoxicology*. 2014;8(4):422–432. doi:10.3109/17435390.2013.796017
18. Chattopadhyay RR. Possible mechanism of hepatoprotective activity of Azadirachta indica leaf extract: part II. *J Ethnopharmacol*. 2003;89 (2–3):217–219. doi:10.1016/j.jep.2003.08.006
19. Jeong HG, You HJ, Park SJ, et al. Hepatoprotective effects of 18β-glycyrrhetinic acid on carbon tetrachloride-induced liver injury: inhibition of cytochrome P450 2E1 expression. *Pharmacol Res*. 2002;46(3):221–227. doi:10.1016/S1043-6618(02)00121-4
20. Ricci D, Giamperi L, Bucchini A, Fraternale D. Antioxidant activity of Punica granatum fruits. *Fitoterapia*. 2006;77(4):310–312. doi:10.1016/j.fitote.2006.01.008
21. Lansky E, Shubert S, Neeman I, editors. Pharmacological and therapeutic properties of pomegranate. Symposium on production, processing and marketing of pomegranate in the Mediterranean region: advances in research and technology Séminaires Méditerranéens (CIHEAM) PP; 2000. Orihuela (Spain).
22. Karimi M, Sadeghi R, Kokini J. Pomegranate as a promising opportunity in medicine and nanotechnology. *Trends Food Sci Tech*. 2017;69:59–73. doi:10.1016/j.tifs.2017.08.019

23. Cerdá B, Cerón JJ, Tomás-Barberán FA, Espín JC. Repeated oral administration of high doses of the pomegranate ellagitannin punicalagin to rats for 37 days is not toxic. *J Agric Food Chem*. 2003;51(11):3493–3501. doi:10.1021/jf020842c
24. Chidambara Murthy KN, Jayaprakasha GK, Singh RP. Studies on antioxidant activity of pomegranate (Punicagranatum) peel extract using in vivo models. *J Agric Food Chem*. 2002;50(17):4791–4795. doi:10.1021/jf0255735
25. Faria A, Calhau C, de Freitas V, Mateus N. Procyanidins as antioxidants and tumor cell growth modulators. *J Agric Food Chem*. 2006;54(6):2392–2397. doi:10.1021/jf0526487
26. Luna IZ, Hilary LN, Chowdhury AS, et al. Preparation and characterization of copper oxide nanoparticles synthesized via chemical precipitation method. *Open Access Lib J*. 2015;2(03):1.
27. Faria A, Monteiro R, Mateus N, Azevedo I, Calhau C. Effect of pomegranate (Punica granatum) juice intake on hepatic oxidative stress. *Eur J Nutr*. 2007;46(5):271–278. doi:10.1007/s00394-007-0661-z
28. Albus U. *Guide for the Care and Use of Laboratory Animals*. 8th ed. SAGE Publications Sage UK: London, England; 2012.
29. Guardado-Mendoza R, Prioletta A, Jiménez-Ceja LM, Sosale A, Folli F. The role of nateglinide and repaglinide, derivatives of meglitinide, in the treatment of type 2 diabetes mellitus. *Arch Med Sci*. 2013;9(5):936. doi:10.5114/aoms.2013.34991
30. Chakraborty M, Ahmed MG, Bhattacharjee A. Potential pharmacodynamic and pharmacokinetic interaction of pomegranate juice and nateglinide against diabetes induced complications in rats. *Synergy*. 2017;5:1–6. doi:10.1016/j.synres.2017.11.002
31. Doudi M, Setorki M. Acute effect of nano-copper on liver tissue and function in rat. *Nanomed J*. 2014;1(5).
32. Bancroft JD. *Histochemical Techniques*. Butterworth-Heinemann; 2013.
33. Khalaf AA, Hassanen EI, Zaki AR Tohamy AF, Ibrahim MA. Histopathological, immunohistochemical, and molecular studies for determination of wound age and vitality in rats. Inter wound j. 2019. doi.org/10.1111/iwj.13206
34. BALIGA R, UEDA N, WALKER PD, SHAH SV. Oxidant mechanisms in toxic acute renal failure. *Drug Metab Rev*. 1999;31(4):971–997. doi:10.1081/DMR-100101947
35. Ohkawa H, Ohishi N, Yagi K. Assay for lipid peroxides in animal tissues by thiobarbituric acid reaction. *Anal Biochem*. 1979;95(2):351–358. doi:10.1016/0003-2697(79)90738-3
36. Beutler E. Improved method for the determination of blood glutathione. *J Lab Clin Med*. 1963;61:882–888.
37. Abdel-Aziz RL, Abdel-Wahab A, El-Ela FIA, et al. Dose-dependent ameliorative effects of quercetin and l-Carnitine against atrazine-induced reproductive toxicity in adult male Albino rats. *Biomed Pharmcother*. 2018;102:855–864. doi:10.1016/j.biopha.2018.03.136
38. Khalaf A, Ahmed W, Moselhy W, Abdel-Halim B, Ibrahim M. Protective effects of selenium and nano-selenium on bisphenol-induced reproductive toxicity in male rats. *Hum Exp Toxicol*. 2019;38(4):398–408. doi:10.1177/0960327118816134
39. Zheng W, Jiang Y-M, Zhang Y, et al. Chelation therapy of manganese intoxication with para-aminosalicylic acid (PAS) in Sprague–Dawley rats. *Neurotoxicology*. 2009;30(2):240–248. doi:10.1016/j.neuro.2008.12.007
40. Khalid S, Afzal N, Khan JA, et al. Antioxidant resveratrol protects against copper oxide nanoparticle toxicity in vivo. *Naunyn Schmiedebergs Arch Pharmacol*. 2018;391(10):1053–1062. doi:10.1007/s00210-018-1526-0
41. Sangha G, Kaur K. Cypermethrin lnduced changes in biochemical constituents of plasma of female albino rats. *Indian J Anim Res*. 2011;45(3):186–191.
42. Xu P, Xu J, Liu S, Yang Z. Nano copper induced apoptosis in podocytes via increasing oxidative stress. *J Hazard Mater*. 2012;241:279–286. doi:10.1016/j.jhazmat.2012.09.041
43. Wang J-X, Fan Y-B, Gao Y, Hu Q-H, Wang T-C. TiO_2 nanoparticles translocation and potential toxicological effect in rats after intraarticular injection. *Biomaterials*. 2009;30(27):4590–4600. doi:10.1016/j.biomaterials.2009.05.008
44. Ma L, Zhao J, Wang J, et al. The acute liver injury in mice caused by nano-anatase TiO_2. *Nanoscale Res Lett*. 2009;4(11):1275. doi:10.1007/s11671-009-9393-8
45. Sadauskas E, Wallin H, Stoltenberg M, et al. Kupffer cells are central in the removal of nanoparticles from the organism. *Part Fibre Toxicol*. 2007;4(1):10. doi:10.1186/1743-8977-4-10
46. Wang Z, Li N, Zhao J, et al. CuO nanoparticle interaction with human epithelial cells: cellular uptake, location, export, and genotoxicity. *Chem Res Toxicol*. 2012;25(7):1512–1521. doi:10.1021/tx3002093
47. Møller P, Jacobsen NR, Folkmann JK, et al. Role of oxidative damage in toxicity of particulates. *Free Radic Res*. 2010;44(1):1–46.
48. Fahmy B, Cormier SA. Copper oxide nanoparticles induce oxidative stress and cytotoxicity in airway epithelial cells. *Toxicol In Vitro*. 2009;23(7):1365–1371. doi:10.1016/j.tiv.2009.08.005
49. Hockenbery DM, Oltvai ZN, Yin X-M, Milliman CL, Korsmeyer SJ. Bcl-2 functions in an antioxidant pathway to prevent apoptosis. *Cell*. 1993;75(2):241–251. doi:10.1016/0092-8674(93)80066-N
50. Wang T, Chen X, Long X, Liu Z, Yan S. Copper nanoparticles and copper sulphate induced cytotoxicity in hepatocyte primary cultures of Epinephelus coioides. *PLoS One*. 2016;11(2):e0149484. doi:10.1371/journal.pone.0149484
51. Sarkar A, Das J, Manna P, Sil PC. Nano-copper induces oxidative stress and apoptosis in kidney via both extrinsic and intrinsic pathways. *Toxicology*. 2011;290(2–3):208–217. doi:10.1016/j.tox.2011.09.086
52. Nel A, Xia T, Mädler L, Li N. Toxic potential of materials at the nanolevel. *Science*. 2006;311(5761):622–627. doi:10.1126/science.1114397
53. Hu R, Zheng L, Zhang T, et al. Molecular mechanism of hippocampal apoptosis of mice following exposure to titanium dioxide nanoparticles. *J Hazard Mater*. 2011;191(1–3):32–40. doi:10.1016/j.jhazmat.2011.04.027
54. Jiang J, Wang J, Zhang X, et al. Activation of mitogen-activated protein kinases cellular signal transduction pathway in mammalian cells induced by silicon carbide nanowires. *Biomaterials*. 2010;31(31):7856–7862. doi:10.1016/j.biomaterials.2010.07.024
55. Suliman A, Lam A, Datta R, Srivastava RK. Intracellular mechanisms of TRAIL: apoptosis through mitochondrial-dependent and-independent pathways. *Oncogene*. 2001;20(17):2122. doi:10.1038/sj.onc.1204282
56. Laha D, Pramanik A, Maity J, et al. Interplay between autophagy and apoptosis mediated by copper oxide nanoparticles in human breast cancer cells MCF7. *Biochim Biophys Acta Bioenerg*. 2014;1840(1):1–9. doi:10.1016/j.bbagen.2013.08.011
57. An L, Liu S, Yang Z, Zhang T. Cognitive impairment in rats induced by nano-CuO and its possible mechanisms. *Toxicol Lett*. 2012;213(2):220–227. doi:10.1016/j.toxlet.2012.07.007
58. Siddiqui MA, Alhadlaq HA, Ahmad J, et al. Copper oxide nanoparticles induced mitochondria mediated apoptosis in human hepatocarcinoma cells. *PLoS One*. 2013;8(8):e69534. doi:10.1371/journal.pone.0069534
59. Semisch A, Ohle J, Witt B, Hartwig A. Cytotoxicity and genotoxicity of nano-and microparticulate copper oxide: role of solubility and intracellular bioavailability. *Part Fibre Toxicol*. 2014;11(1):10. doi:10.1186/1743-8977-11-10
60. Sen R, Baltimore D. Multiple nuclear factors interact with the immunoglobulin enhancer sequences. *cell*. 1986;46(5):705–716. doi:10.1016/0092-8674(86)90346-6
61. Garg A, Aggarwal B. Nuclear transcription factor-κB as a target for cancer drug development. *Leukemia*. 2002;16(6):1053.
62. Smith KR, Klei LR, Barchowsky A. Arsenite stimulates plasma membrane NADPH oxidase in vascular endothelial cells. *Am J Physiol Lung Cell Mol Physiol*. 2001;280(3):L442–L9. doi:10.1152/ajplung.2001.280.3.L442

63. Thannickal VJ, Fanburg BL. Reactive oxygen species in cell signaling. *Am J Physiol Lung Cell Mol Physiol*. 2000;279(6):L1005–L28. doi:10.1152/ajplung.2000.279.6.L1005
64. Allen R, Tresini M. Oxidative stress and gene regulation. *Free Radical Biol Med*. 2000;28(3):463–499. doi:10.1016/S0891-5849(99)00242-7
65. Byrne JD, Baugh JA. The significance of nanoparticles in particle-induced pulmonary fibrosis. *Mcgill J Med*. 2008;11(1):43.
66. Murray AR, Kisin ER, Tkach AV, et al. Factoring-in agglomeration of carbon nanotubes and nanofibers for better prediction of their toxicity versus asbestos. *Part Fibre Toxicol*. 2012;9(1):10. doi:10.1186/1743-8977-9-10
67. Medjakovic S, Jungbauer A. Pomegranate: a fruit that ameliorates metabolic syndrome. *Food Funct*. 2013;4(1):19–39.
68. Yehia HM, Elkhadragy MF, Moneim AEA. Antimicrobial activity of pomegranate rind peel extracts. *Afr J Microbiol Res*. 2011;5(22):3664–3668.
69. Lansky EP, Harrison G, Froom P, Jiang WG. Pomegranate (Punica granatum) pure chemicals show possible synergistic inhibition of human PC-3 prostate cancer cell invasion across Matrigel™. *Invest New Drugs*. 2005;23 (2):121–122. doi:10.1007/s10637-005-5856-7
70. Van Elswijk DA, Schobel UP, Lansky EP, Irth H, van der Greef J. Rapid dereplication of estrogenic compounds in pomegranate (Punica granatum) using on-line biochemical detection coupled to mass spectrometry. *Phytochemistry*. 2004;65(2):233–241. doi:10.1016/j.phytochem.2003.07.001
71. Schubert SY, Lansky EP, Neeman I. Antioxidant and eicosanoid enzyme inhibition properties of pomegranate seed oil and fermented juice flavonoids. *J Ethnopharmacol*. 1999;66(1):11–17. doi:10.1016/S0378-8741(98)00222-0
72. Abdel Moneim AEA, El-Khadragy MF. The potential effects of pomegranate (Punica granatum) juice on carbon tetrachloride-induced nephrotoxicity in rats. *J Physiol Biochem*. 2013;69(3):359–370. doi:10.1007/s13105-012-0218-3
73. Coballase-Urrutia E, Pedraza-Chaverri J, Cárdenas-Rodríguez N, et al. Hepatoprotective effect of acetonic and methanolic extracts of Heterotheca inuloides against CCl4-induced toxicity in rats. *Exp Toxicol Pathol*. 2011;63(4):363–370. doi:10.1016/j.etp.2010.02.012
74. Raja S, Ahamed KN, Kumar V, et al. Antioxidant effect of Cytisus scoparius against carbon tetrachloride treated liver injury in rats. *J Ethnopharmacol*. 2007;109(1):41–47. doi:10.1016/j.jep.2006.06.012
75. Yuan L, Chen F, Ling L, et al. Protective effects of total flavonoids of Bidens bipinnata L. against carbon tetrachloride-induced liver fibrosis in rats. *J Pharm Pharmacol*. 2008;60(10):1393–1402.
76. Lin H-M, Tseng H-C, Wang C-J, et al. Hepatoprotective effects of Solanum nigrum Linn extract against CCl4-induced oxidative damage in rats. *Chem Biol Interact*. 2008;171(3):283–293. doi:10.1016/j.cbi.2007.08.008
77. Larrosa M, González-Sarrías A, Yáñez-Gascón MJ, et al. Anti-inflammatory properties of a pomegranate extract and its metabolite urolithin-A in a colitis rat model and the effect of colon inflammation on phenolic metabolism. *J Nutr Biochem*. 2010;21(8):717–725. doi:10.1016/j.jnutbio.2009.04.012
78. de Nigris F, Balestrieri ML, Williams-Ignarro S, et al. The influence of pomegranate fruit extract in comparison to regular pomegranate juice and seed oil on nitric oxide and arterial function in obese Zucker rats. *Nitric Oxide*. 2007;17(1):50–54. doi:10.1016/j.niox.2007.04.005
79. Rasheed Z, Akhtar N, Anbazhagan AN, et al. Polyphenol-rich pomegranate fruit extract (POMx) suppresses PMACI-induced expression of pro-inflammatory cytokines by inhibiting the activation of MAP Kinases and NF-κB in human KU812 cells. *J Inflamm*. 2009;6(1):1. doi:10.1186/1476-9255-6-1